

MORPHOLOGICAL SEGMENTATION OF REMOTELY SENSED FOREST COVERS IN HIGH SPATIAL RESOLUTION IMAGES

T. BARATA, P. PINA

*CVRM / Centro de Geo-Sistemas, Instituto Superior Técnico
Av. Rovisco Pais, 1049-001 Lisboa, PORTUGAL*

Abstract In this paper novel algorithms developed to automatically segment forest cover types are presented. The digital image analysis followed is mainly based on mathematical morphology operators and exploits the textural features in high spatial resolution images. These input images consist of true colour digital orthophotos and the studied forest covers consist of the main occurrences in Portugal: olive trees, cork oak trees, pine and eucalyptus trees.

Keywords: Segmentation, textural features, forest covers, high spatial resolution images.

1. Introduction

The objective of image segmentation can be simply stated as the definition of homogeneous zones according to some criteria [17]. There exists in the literature a great variety of approaches developed over the years to attend this purpose, some are more general, others are highly dedicated (good overview in [14]). Specifically, in its application in remotely sensed images representing Earth's surface [8, 11], the benefit from important theoretical and technical advances, exploiting not only spectral but also textural information has been very important in the last decades but has left intact some difficulties that are far from being solved. Presently, with the latest generation of satellites providing an easier access to images with higher spatial resolution, the "excuse" for not using its textural features is no longer acceptable. In these high spatial resolution images not only the details at human scale can now be observed clearly but also "new" spatial patterns can now be detected as, for instance, the ones exhibited by some forest covers. But if one thing is to "see" the details clearly another one is to identify them automatically. These features can highly contribute to a more correct automatic identification once for some forest covers the high similarity of its spectral behaviors does not allow a good discrimination. The segmentation of remotely sensed images has been proposed

for several different vegetation and forest covers with a certain success in some test regions [9, 10, 13] but without making explicit the degree of confidence in routine application of automatic upgrading procedures of forest covers.

2. Methods and algorithms

In morphological segmentation procedures emerge, among others, the watershed [3] and the top-hat [12] transforms. The direct use of these transforms or the construction of other more elaborated ones using morphological elementary operators seem to be a good option to exploit, among the set of several digital image analysis methods, when geometrical or textural features of images are to be considered. The most frequent forest cover types that occur in Portugal are the olive, cork oak, pine and eucalyptus trees being the key-idea to explore the particular textural patterns exhibited: olive trees present a highly regular pattern over straight lines and rows (figure 1a); cork oak trees appear randomly without particular patterns but normally occur isolated or creating clusters with a certain degree of overlapping that still allow the perception of individual trees (figure 2a); pine and eucalyptus trees occur commonly in compact and large dark regions, often mixed, with highly irregular shapes and contours where the perception of individual trees is rather difficult to detect (figure 3a).

The development of a methodology to automatically segment these forest covers in high spatial resolution images (orthophotomaps) based on its individual textural features and appealing mainly to mathematical morphology operators, using important hints given by a previous work [6], is then presented in the following. The digital input images are true colour ones (RGB) with a dimension of 2500 x 2500 pixels, being each cover type segmented separately over the Hue-Intensity-Saturation converted images, each one with 256 gray levels digitized with a spatial resolution of 1 metre/pixel.

2.1 OLIVE TREES

Olive trees are characterized by presenting similar circular and dark cupolas constructing regular patterns on lighter backgrounds. These patterns exhibit a high degree of regularity along lines and rows because, for agricultural practices, the distance between the trees is standard (figure 1a). Moreover, the land where these trees are located is seasonally cleaned, showing this way homogeneous bare or almost bare soil.

The olive trees can be segmented using the top-hat transform introduced in its black or valley version, since it identifies the local darker regions over a lighter background independently from its height location. The direct application of the black top hat transform, $BTH(f)$, segments not only the desired sets of trees but, besides some noise, the darker regions of the image that have the same size, *i.e.*, the valleys that correspond to directional structures like roads, water lines, or connected alignment of trees. No matter how long these structures are, they are always detected if present their thickness is smaller

than the diameter of the structuring element used. In figure 1b is presented an application of the black top hat transform, where the dark structures that have a size smaller or equal to the structuring element are segmented: it consists of the olive trees, some isolated trees (mainly cork oak type), some continuously aligned trees (see the structure along the road in white that starts at the bottom left corner of the image in 1a), and some bushes and vegetation. In order to avoid the segmentation of directional or aligned structures, the top hat transform should be modified. The modified transform is based on the one proposed by Lay [7] to segment small black spots in the human retina. It consists of firstly computing the *inf* of the directional closings of the initial image f in the main directions of the digital grid used (in the hexagonal case the directions α , $\alpha + 60^\circ$ and $\alpha + 120^\circ$ are the ones used) with directional structuring elements l of the maximum diameter λ of the trees, followed by the difference between this image and the initial one f , thresholded T at adequate levels (t_1 and t_2):

$$X_1 = \text{IBTH}(f) = T[\text{inf}(\varphi^{\lambda l}(f, \alpha), \varphi^{\lambda l}(f, \alpha + 60^\circ), \varphi^{\lambda l}(f, \alpha + 120^\circ)) - f] \quad (1)$$

The result of the application of this isotropic black top-hat transform, $\text{IBTH}(f)$ can be seen in figure 1c. The differences between this image and one resulting from the application of the classic top-hat transform are evident: only the isotropic dark structures are now segmented, resulting in a cleaner image.

To filter now the remaining undesirable structures one has to take advantage of the regular pattern exhibited by the olive trees. The filtering of non-olive trees is done in the following main steps: (i) pre-filtering and creation of a cluster or mask that contains the olive trees; (ii) filtering the structures outside the mask and (iii) filtering the structures inside the mask. The pre-filtering consists of suppressing the small noisy structures that are not trees by application of an opening γ of small size. In figure 1d is presented the result of the application of an opening of size 1:

$$X_2 = \gamma^{\lambda B}(X_1) \quad (2)$$

The creation of a cluster of olive trees can be obtained by a closing operation with an isotropic structuring element of half of the size of the distance between adjacent trees in a line or row of the regular pattern (figure 1e):

$$X_3 = \varphi^{\lambda/2B}(X_2) \quad (3)$$

This strong cluster is now able to resist erosion-reconstruction filters. The application of an erosion ε with an isotropic element will remove the smaller unwanted structures and will leave some regions that belong to the mask of the olive trees:

$$X_4 = \varepsilon^{\lambda B}(X_3) \quad (4)$$

In figure 1f is shown the application of an erosion ε with a hexagon λB where the external structures to the olive trees are suppressed and where only some

regions of the mask have resisted to this transform. These regions X_4 will serve now as markers for the reconstruction R of the final mask (set X_5) in the X_3 :

$$X_5 = R_{X_3}(X_4) = \delta_{X_3}^\infty(X_4) \quad (5)$$

The output of this transform can be seen in figure 1g. The set intersection of X_1 and X_5 will provide as result the olive trees (set X_6) and also some unwanted structures located between the trees, that still have to be filtered (figure 1h):

$$X_6 = X_1 \cap X_5 \quad (6)$$

In order to filter the structures inside the mask, *i.e.*, to leave only the regions that correspond to olive trees a morphological algorithm is presently being developed.

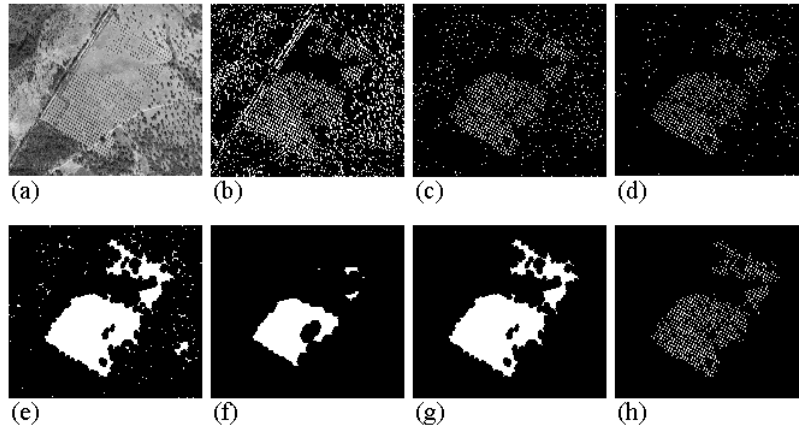


Figure 1. Olive tree segmentation sequence: (a) Initial image (intensity component); (b) Classic black top-hat of (a); (c) Isotropic black top-hat of (a); (d) Opening of (c); (e) Closing of (d); (f) Erosion of (e); (g) Reconstruction of (f) in (e); (h) Intersection between (g) and (c) (final result).

2.2 CORK OAK TREES

Cork oak trees have, in general, larger circular cupolas and do not present a spatial regular pattern like the one exhibited by the olive trees. In some regions the trees appear more concentrated, creating somehow clusters with a certain degree of overlapping of the cupolas, in other regions the dispersion is very high with isolated trees very far from its closest neighbor trees. Moreover, the land over which the cork oak trees occur is highly variable: bare soils of different constitutions and soils with different types and densities of low vegetation are frequent. Thus, these different features directly reflected in the images make it difficult to define a typical pattern for this forest cover type (some of these details can be seen in figure 2b). Consequently, besides exploiting the textural

features of the images, spectral information is also very helpful. The solution comes from using image(s) where the cork oak trees exhibit the same type of behavior according to the soil or vegetation around it, *i.e.*, the trees should always be lighter (or darker) than the surrounding land classes or background. By analysing the Hue-Saturation-Intensity (HIS) colour space it is noticed that in the Saturation component (figure 3b) the trees present much higher values than bare soil and higher values than vegetation or mixed soil. These higher saturation values are due not only to the intrinsic features of the leaves of the trees but also to its compact spatial arrangement, which does not occur in soils with vegetation where compactness is not always as high as in the trees. Then, cork oak trees can be segmented firstly on the Hue channel, f_H , through a white top-hat transform [12], $WTH(f_H)$:

$$X_1 = WTH(f_H) = T[f_H - \gamma^{\lambda B}(f_H)]_{t_1, t_2} \quad (7)$$

that consists of thresholding at levels t_1 and t_2 the gray level image resulting from the numerical difference between the original image f_H and the opened image $\gamma(f_H)$ with the structuring element λB . An example of the application of this transform is shown in figure 2d, where it is noticeable that the trees are segmented together with unwanted structures, not only derived from white local regions (peaks) over the background but also from the shadows of the trees.

The size of the shadows of the trees not only depends on the size of the trees but also on the position of the sun on the horizon, varying in the images from region to region, depending on the daily time that the aerial photograph was taken. But in terms of spectral response its behavior is very constant in the Saturation channel (f_S). The application of a white top-hat transform of smaller dimension than the one used for detecting the cork oak trees allows the extraction of the shadows (set X_2 , figure 2e):

$$X_2 = WTH(f_S) = T[f_S - \gamma^{\lambda B}(f_S)]_{t_1, t_2} \quad (8)$$

The filtering procedures start by performing the set difference between these two binary images (X_1 and X_2) (figure 2f):

$$X_3 = X_1 \setminus X_2 \quad (9)$$

followed by an erosion in order to remove the structures not corresponding to trees (figure 2g) and to the re-positioning of the original shape of the remaining structures of the cork oak trees by a reconstruction R of the marker set X_4 in the geodesics X_3 :geodesics

$$X_4 = R_{X_3}[\varepsilon(X_3)] \quad (10)$$

In order to filter the transition regions between the trees and its shadows or between the shadows and the background (normally bare soil or vegetation) that correspond to thin regions with intermediate gray levels between these regions, the application of an opening of small dimension is sufficient and leads to the final result (figure 2h):

$$X_5 = \gamma^{\lambda B}(X_4) \quad (11)$$

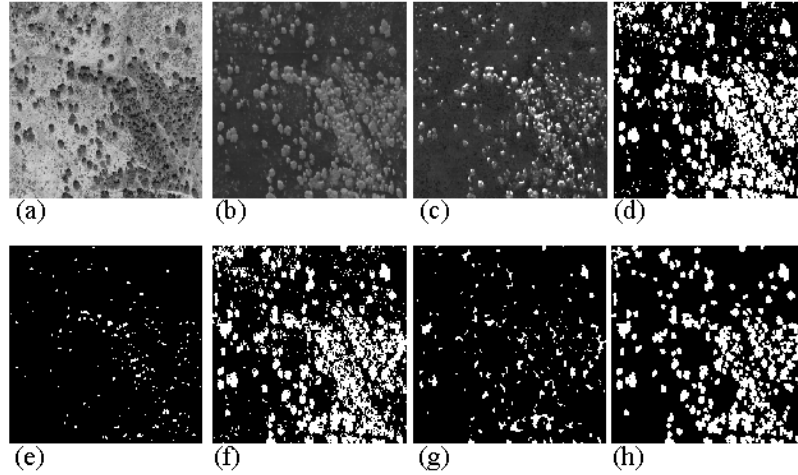


Figure 2. Cork oak tree segmentation sequence: (a) Intensity channel; (b) Hue channel; (c) Saturation channel; (d) White top-hat on the Hue image; (e) White top-hat on the Saturation image; (f) Difference between (d) and (e); (g) Erosion of (f); (h) Reconstruction of (g) in (f) followed by an opening (final result).

2.3 PINE AND EUCALYPTUS TREES

Unfortunately, due to unsatisfying past territorial planning, pine and eucalyptus trees areas do not appear in pure regions but are very often mixed, presenting very similar intensity levels in any spectral band or channel. The cupola shapes and the spatial pattern presented by the implantation of trees are also not very discriminating features. Presently, the areas of pine and eucalyptus trees have been kept together in the same class due to their high degree of mixing in the region under study and can be characterized as great dark regions with irregular contours and presenting infinite shapes. Thus, the algorithm developed pursues the objective of detecting the contours of great valleys that correspond to these forest cover classes. The final objective of this algorithm is to apply the watershed transform [3], with its most recent improvements (modification of the homotopy with imposition of internal markers on the gradient image [4, 5]), being the effort put on its development on the preparation of adequate images to be segmented, *i.e.*, images where great valleys correspond to the referred forest cover classes.

The developed algorithm operates on the intensity images (figure 3a). Although large dark regions are noticeable, the existence of a large number of local topographic irregularities (local peaks and valleys) will produce over-segmented images if the watershed transform is directly applied. In order to create flatter valleys, the local topographic depressions (smaller valleys) that correspond in most of the situations to dispersed or isolated trees have to be filled. This

procedure starts by its identification through a black top hat transform of the intensity image f :

$$X_1 = \text{BTH}(f_H) = T[\varphi^{\lambda B}(f) - f]_{t_1, t_2} \quad (12)$$

These valleys (figure 3b) are located at different heights. Thus, in order to respect its local topographies the valley filling operation is performed through a dual reconstruction R^* of the following image f_1 (marker function) into the function f (mask or geodesics function):

$$f_1 = \begin{cases} 255 & x \in X_1 \\ f & x \in X_1^c \end{cases} \quad (13)$$

This operation converts the points x that mainly correspond to dispersed trees (small valleys) into the highest value allowed (255) (given by set X_1) while the other regions (complementary set X_1^c) have the values of the initial image f . In the following, the dual reconstruction of the marker function f_1 into the mask function f :

$$f_2 = R_f^*(f_1) \quad (14)$$

produces a new image f_2 where the small dimension valleys are now filled (figure 3c). This image f_2 is now the object of a filtering procedure in order to create larger regions (dark or bright). The alternating sequential filter (ASF) [16] that alternates sequences of openings and closings of increasing dimension seem adequate to reach those objective, as the example of figure 3d shows. The application of an ASF of closing-opening type (the sequence starts by an opening):

$$f_3 = [\varphi\gamma]_i = \gamma_i\varphi_i\dots\varphi_3\gamma_3\gamma_2\varphi_2\varphi_1\gamma_1(f_2) \quad (15)$$

enhances lighter regions like bare soil and darker regions like eucalyptus and pine trees in the centre of figure 3d. This flatter image will be now used for computing the crest lines through the watershed transform. The morphological gradient of f_3 (figure 3e):

$$f_4 = \text{grad}(f_3) = \delta^{\lambda B}(f_3) - \varepsilon^{\lambda B}(f_3) \quad (16)$$

and its minima, *i.e.*, the set of points that mark both dark and bright large regions (figure 3f):

$$X_2 = \text{min}(f_4) \quad (17)$$

are used to compute the watershed transform:

$$X_3 = \text{Wsh}_{X_2}(f_4) \quad (18)$$

The resulting partition that divides the complete image into several catchment basins is presented in figure 3g. It is now necessary to identify the ones

that correspond to the cover type under study. The catchment basins image is simply the complementary image of the watershed lines:

$$X_4 = CB(f_4) = (X_3)^c \quad (19)$$

Since the eucalyptus and pine trees present a low gray level value in the intensity image, the minimum that marks each catchment basin also has the same behavior. By introducing an adequate thresholding on the computation of the minima in order to select the ones located at lower height, it is possible to construct an image containing only the minima that mark catchment basins that correspond to eucalyptus and pine trees regions (figure 3h):

$$X_5 = T[grad(f_2)]_{t_1, t_2} \quad (20)$$

A simple set reconstruction of these sets of minima into the catchment basins set (complementary set of the watershed lines) gives the image containing only the desired regions. The application of an isotropic closing φ of size 1 merges the adjacent basins into a larger basin:

$$X_6 = \varphi^{1B}[R_{X_4}(X_5)] \quad (21)$$

The internal regions or holes detected are due to some local peaks in the gray level image. Since its number seems exaggerated, a filtering procedure is still envisaged. Analysing carefully the original images, some of these holes correspond to bare soil regions or to regions where locally there are no eucalyptus or pine trees. It was then decided to fill these regions according to its size, *i.e.*, to fill the smaller ones and to leave intact the larger ones. An erosion-reconstruction of the complementary set of X_6 , followed by their complementation, performs this task:

$$X_7 = [R_{X_6}(\varepsilon^{\lambda B}(X_6))]^c \quad (22)$$

The size λ of the structuring element B in the erosion operation determines the size of the hole to be filled. Figure 3i presents the region with holes filled up to a dimension of 3 metres.

3. Conclusions and future developments

In this paper three different algorithms to automatically segment the 4 main forest cover types that occur in Portugal (olive, cork oak, pine and eucalyptus trees) are presented. These algorithms exploit the textural features presented by each cover type, appealing to mathematical morphology operators. The results obtained on the application of these algorithms in a centre region in Portugal, although highly satisfying, still face some difficulties that are presently being the subject of improvement. These actions should exploit with more detail the textural features of the images, incorporate ancillary information (digital terrain models, cartographic information) and use some spectral information in order to overcome or attenuate some unsolved problems related to similarity of the regular patterns (for instance, between olive and some fruit trees), to the occurrence of some unclustered large trees that may be confused

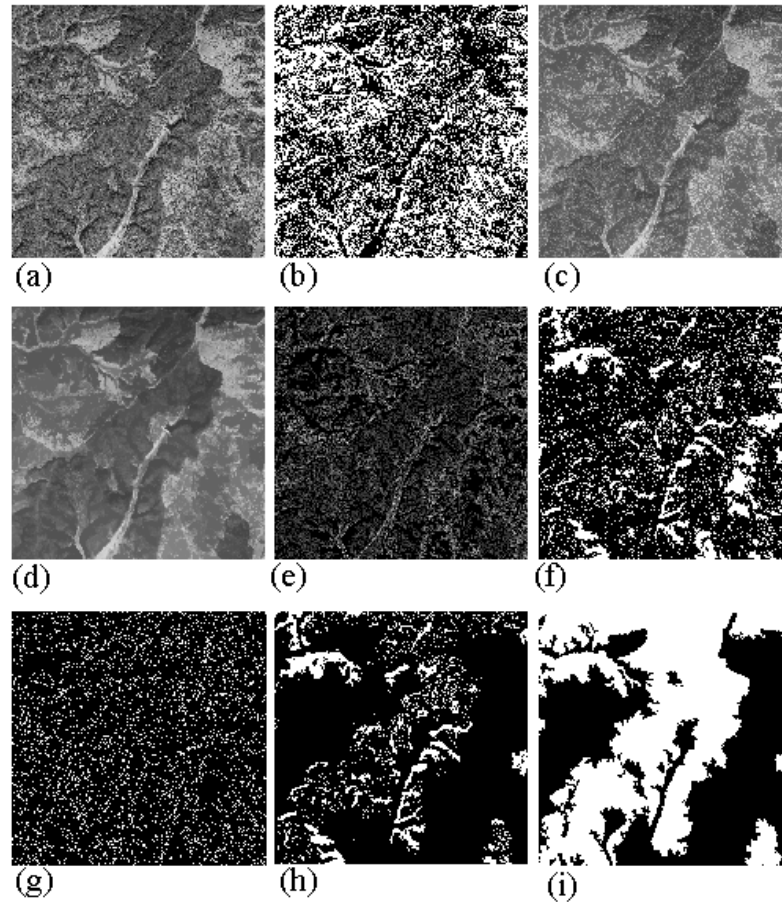


Figure 3. Pine and eucalyptus segmentation sequence: (a) Intensity channel; (b) Black top-hat; (c) Valley filling (reconstruction); (d) ASF of closing-opening type; (e) Morphological gradient of (d); (f) Minima of (e); (g) Watershed of (e) using (f) as markers; (h) Lower height minima; (i) Reconstruction of (h) in the complementary set of (g) and selective hole filling.

with the cork oak trees and to the presence of low spatial density regions of pine and eucalyptus (young trees or existence of recent cuts).

References

- [1] T. Barata, P. Pina, I. Granado. Segmenting at higher scales to classify at lower scales. A mathematical morphology based approach applied to forest cover remote sensing images. In A. Sanfeliu, J.J. Villanueva, M. Vanrell, R. Alquzar, J. Crowley and Y. Shirai, editors, *Proceedings of ICPR'2000 - 15th International Conference on Pattern Recognition-Barcelona, Spain*, vol.4, pages 84-87, Los Alamitos, California, 2000. IEEE Computer Society.

- [2] T. Barata. Classification of forest covers in remotely sensed images through a mathematical morphology based methodology (in portuguese). PhD thesis, Technical University of Lisboa, Lisboa, 2001.
- [3] S. Beucher, Ch. Lantuéjoul. Use of watersheds in contour detection. *Proc. Int. Workshop on Image Processing: Real-Time Edge and Motion Detection/Estimation*, Rennes, 1979.
- [4] S. Beucher. Segmentation d'images et morphologie mathématique. Thèse de doctorat, ENSMP, Paris, 1990.
- [5] S. Beucher, F. Meyer. The morphological approach to segmentation: The watershed transformation. In E. Dougherty, editor, *Mathematical Morphology in Image Processing*, pages 433–482, New York, 1993. Marcel Dekker.
- [6] I. Granado, M. Mengucci, T. Barata, F. Muge. Automatic classification of forest land use on ortho-images using mathematical morphology approach. In J.R. Shulcloper, J.F. Martinez Trinidad, G. Sánchez Diaz, J.A. Carrasco Ochoa, S. Muñoz Gutierrez and W. Mayol Cuevas, editors, *Memorias SIARP'99 - 4th Iberian Conference on Pattern Recognition*, pages 389–398, Havana, Cuba, 1999.
- [7] B. Lay. Analyse automatique des images angiofluorographiques. Thèse de doctorat, ENSMP, Paris, 1983.
- [8] T.M. Lillesand, R.W. Kiefer. *Remote sensing and image interpretation*. 4th edition, J. Wiley and Sons, New York, 2000.
- [9] A. Lobo. Image segmentation and discriminant analysis for the identification of landscape units in ecology. *IEEE Transactions on Geoscience and Remote Sensing*, 35(5):1136–1145, 1997.
- [10] A. Lobo, K. Moloney, N. Chiariello. Fine-scale mapping of grassland from digitized aerial photographs: an approach using image segmentation and discriminant analysis. *International Journal of Remote Sensing*, 19(1):65–84, 1998.
- [11] P. Mather. *Computer processing of remotely-sensed images. An introduction*. 2nd edition, J. Wiley and Sons, New York, 1999.
- [12] F. Meyer. Cytologie quantitative et morphologie mathématique. Thèse de doctorat, ENSMP, Paris, 1979.
- [13] P.L. Palmer, M. Petrou. Locating boundaries of textured regions. *IEEE Transactions on Geoscience and Remote Sensing*, 35(5):1367–1371, 1997.
- [14] J.C. Russ. *The handbook of image processing*. 3rd edition, CRC Press and Springer Verlag, Boca Raton and Heidelberg, 1999.
- [15] J. Serra. *Image analysis and mathematical morphology*. Academic Press, London, 1982.
- [16] J. Serra (ed). *Image analysis and mathematical morphology, vol.2: Theoretical advances*. Academic Press, London, 1988.
- [17] P. Soille. *Morphological image analysis*. Springer, Berlin, 1999.